Nonlinear Vortex Interactions on Wing-Canard Configurations

DAVID FINKLEMAN*
Frank J. Seiler Research Laboratory, U.S. Air Force Academy, Colo.

Sacks' method of simulating vortex sheets with distributions of discrete vortices has been applied to the study of the interaction of a slender wing with a nearby canard surface. The canard is detrimental to both lift and static longitudinal stability. The extent of canard vortex sheet rollup is very important in the interaction. Downward canard deflection may lead to increased lift. For small vertical separations between the surfaces, the forward portion of a pointed wing preceded by a canard is ineffective in producing lift.

Nomenclature

AR = aspect ratio
C_m = moment coefficient about wing apex
C_N = normal force coefficient
C = chord
N = normal force
S_h = horizontal separation
S_v = vertical separation
U_∞ = freestream velocity
W = complex potential
X,Y,Z = Cartesian coordinates
α = angle of attack
Γ = circulation, vortex strength
γ = vortex linear density
δ = vortex sheet width, Eq. 7
ζ = crossflow complex variable, $Y + iZ$
ρ = density
σ = transformed complex variable, Eq. 4
ϕ = velocity potential

Introduction

AIRCRAFT pitch control through deflection of horizontal surfaces behind the wing aerodynamic center is detrimental to net lift. Since elevator deflection decreases lift under circumstances which require an increase, canard surfaces are well suited to high maneuverability. STOL requires that controlling moments be accompanied by large useful force increments, and a canard mounted reasonably close to the wing would accomplish this with minimum decrease of static margin. When a canard and wing are close together, their interaction can be used to achieve the alteration in wing loading required of control configured aircraft.[1] One might transfer most of the load to the wing root or spars during high-g maneuvers. Such applications require the analysis of close coupled wing-canard planforms.

Several investigators have examined wing-canard configurations. When vertical separation is small compared with the horizontal distance between the surfaces, the interaction of wing and canard of moderate aspect ratios can be treated adequately with lifting surface theories. Landahl and Stark[2] have applied methods of linearized aerodynamics to a combination of planforms similar to that of the SAAB Viggen. Carlson and Harris[3] assume the wake to be flat for aspect ratios to which lifting surface theories apply. The distance over which the wake rolls up is proportional to AR/C_L, thus wake rollup will be most important for aircraft of low-aspect ratio operating at high lift coefficients.[4] In order to determine the degree of roll up to be expected, Hackett and Evans[5] extended Westwater's fundamental two-dimensional computations.[6,7] They observed that wake deformation is important. When the horizontal separation of the surfaces is large relative to the chord of the leading surface the wake may be assumed to be fully rolled up into a pair of concentrated vortices. Sacks' investigation of vortex interference[8] on slender aircraft employed this assumption using vortex trajectories computed by Rogers.[9] Yager et al.[10] used horseshoe vortex computations to analyze the interaction of a canard and wing of high-aspect ratio. All vortices shed by the canard were incorporated in a single vortex pair which was allowed to deform under the influence of both canard and wing.

There is a void in interacting lifting surface analyses. Investigations to date are restricted either to small vertical separations and flat wakes for high aspect ratio surfaces or to low aspect ratios, large horizontal separations, and fully rolled-up leading surface vortex wakes. The present study considers the intermediate range in which leading surface wake rollup proceeds together with the interaction.

Sharp-edged planforms exhibit separation at or near the leading edge. Polhamus[11] and others offer evidence of the existence of vortex sheets along the edges of slender planforms even at small angles of attack. These vortex sheets play a significant role in the aerodynamics of slender wings and in many cases lead to normal forces which are comparable with those due to the attached flow. To analyze a slender configuration similar to the SAAB Viggen, one must consider the role of leading edge separation. The problem is complicated by the fact that vortex shedding at the leading edge of the wing is influenced by the presence of vortex sheets shed from the leading and trailing edges of the canard. The phenomena expected are illustrated in Fig. 1. The investigation to be described has led to the development of a method for predicting the aerodynamics of slender, close coupled, wing-canard configurations. Leading and trailing edge vortex sheets are allowed to roll-up naturally, and the only

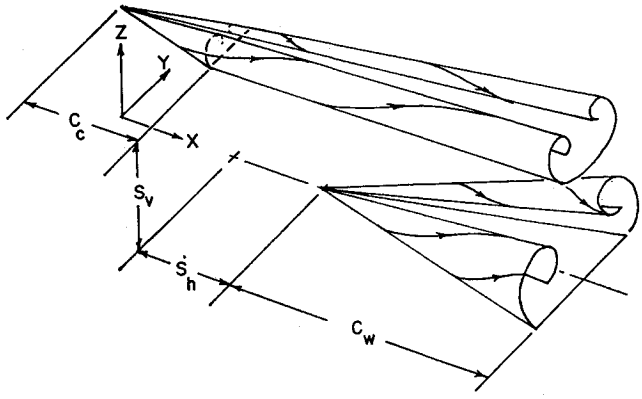

Fig. 1 Delta wing-canard interaction.

Received September 7, 1971; revision received January 20, 1972.
Index categories: Subsonic and Transonic Flow; Aircraft Configuration Design.

* Research Associate and Associate Professor of Aeronautics; presently at Air Force Weapons Laboratory, Laser Research Division, Kirtland Air Force Base, N. Mex. Member AIAA.

restrictions on spacing and planform of the interacting surfaces are those of a slender body theory.

Vortex Separation and Slender Wings

Vortex shedding from both wings and slender bodies may be treated in a unified manner since the physical mechanisms involved in each are the same. Only the location of the separation points and the rates at which vorticity is shed differ between them, and even these differences can be eliminated if longitudinal strakes are placed on the surface of the body.[12] Although stated in the context of slender wings, remarks to follow apply to slender bodies as well. Viscous dissipation is negligible in most situations of interest.

There exist only two distinct methods for analyzing vortex separation. Both are slender body analyses in the Trefftz plane. The method of Brown and Michael[13] approximates leading edge vortex sheets with concentrated vortex cores connected to the edges of the wing by zero strength feeding sheets. Vorticity shed at the wing is convected instantaneously into the core. According to the vortex theorems, the vortex sheet must be a stream surface. It can sustain no force, and the magnitude of the velocity must be continuous across it. The mathematical model cannot satisfy these conditions everywhere since the only unknowns are the strength and location of the vortex core. These are determined by the requirement of smooth outflow at sharp edges which would otherwise be singular points of the complex potential (i.e., a Kutta condition at the wing edges) and the approximation that the feeding sheet—vortex core combination be force free over-all. When conical flow is assumed, vortex position and strength vary linearly along the axis of the wing, and the governing relations become algebraic. Brown and Michael considered only conical flows, but Smith[14] has studied a variety of planforms. Because of the approximations involved, details of the flowfield cannot be predicted. Agreement with experiment is generally not good. Nevertheless, this method has been widely applied, most recently by Kuhn, et. al.[15] to the study of coning of motion of slender bodies.

A generalization of this approach was developed by Mangler and Smith.[16] Their approximation includes a sheet of distributed vorticity which is connected to a concentrated vortex core by a zero strength sheet segment. The Kutta condition at wing edges and the zero force requirement on feeding sheet plus concentrated vortex still provide part of the data required. The numerical treatment requires that the convoluted vortex sheet be broken into segments, and continuity of pressure is required across each segment at its midpoint. The specification of the problem is completed by continuity of normal velocity at each control point. A recent accurate numerical treatment of this method[17] provides great insight into vortex shedding in conical flows. It is found, for instance, that only one convolution of the vortex sheet is often adequate; the remainder of the vorticity being concentrated at the core. Levinsky and Wei[12] have modified the method for application to nonconical flows.

The second method of analyzing vortex separation is due to Sacks, et al.[18] Once the vortex shedding rate is specified, a vortex may be placed at a given chordwise station so as to satisfy the Kutta condition in the presence of vortices previously shed. All vortices are followed to the next chordwise station as they move under their mutual influence in the Trefftz plane. Since it is assured that the vortices follow streamlines, the vortex sheet representation is completely force free. Since vortices may be shed at stations arbitrarily close to each other, the method is exact in the same sense that the Mangler-Smith method is exact. Whereas the latter is numerically inexact in that the vortex sheet is only approximately force free, Sack's method suffers from the fact that the Kutta condition is satisfied only at the chordwise stations at which vortices are shed. Streamline shapes as well as chordwise and spanwise loadings are easily obtained from Sacks' method, but the necessity to follow numerous vortices leads to numerical difficulties. This was the motivation for the study briefly to be described.

Numerical Vortex Tracing

Since it will be necessary to follow the paths of numerous vortices, the numerics of vortex tracing must be examined. Similar analyses are required in the study of vortices in liquid helium[19] and in predicting aircraft wake turbulence.[5] Numerical vortex tracing has been studied for at least 35 years. The earliest published investigations are those of Westwater[6] and Rogers.[9] Both used second-order Euler's method implemented manually, and both warned of unrealistic phenomena which could be expected.

Aerodynamicists often rely upon discrete analogs of continuous distributions of vorticity. A continuous distribution will have an infinite number of spatial moments, some of which are related to physical properties of the vortex system such as its centroid, impulse, and energy. The discrete analog cannot reproduce all of these moments. The velocity field due to the discrete analog will represent that due to the continuous distribution only at distances greater than that spacing between the individual vortices. Whereas the distortions of a continuous vortex sheet can never include crossings of the sheet with itself, the discrete analog is not so restricted because much of the vortex sheet is of zero strength. Since one can hope to preserve only integrated effects of vortex distributions in a numerical investigation, the accuracy of integral properties and not individual vortex locations should be of greatest interest.

The lateral centroid of each half of a symmetric distribution of vortices in a medium without imbedded surfaces is invariant, and the total impulse and energy of the distribution must be preserved.[7] Examination of Westwater's detailed tabulations reveals that the centroid of his ten vortices varied by several percent. During the present investigation several numerical integration schemes were tested for stability and accuracy. Among these were Euler's method, second- and fourth-order predictor-corrector methods of various types, and variations of fourth-order, Runge-Kutta integration. Results of Euler's method for the step sizes noted in the references cited compared favorably with results of Rogers[9] and Westwater.[6] After several time increments, computations with higher order methods predicted significantly different vortex locations. Both single and double precision (48 bit word) computations were performed for up to two hundred vortices in various configurations, and it was observed that, over several thousand time increments, fourth-order, Runge-Kutta integration preserved centroid and impulse to at least eight significant digits. Thus, fourth-order, Runge-Kutta Integration is adequate for the study of the evolution of distributions of numerous vortices.

Detailed Analysis

Smith[22] has documented the most serious shortcomings of Trefftz plane analyses. Slender body theories assume that perturbations to axial velocities are small relative to those in the crossflow. At least in conical flowfields, axial velocities are logarithmically infinite near vortex locations. The inviscid description of a vortex sheet is only a first approximation to the details of vortex separation, and the approximation is certainly not uniformly valid. There are further complications when one attempts to apply the following theory to wings with thickness. These restrictions must be remembered when subsequent results are analyzed.

Most deformable wake studies are performed within the framework of slender body theory. The justification of this approximation is discussed by Ashley and Landahl,[23] and logical extensions have been discussed by Adams and Sears[24] and by Lagerstrom and Graham.[25] For slender wings an expansion in the parameter $\varepsilon = (|1 - M^2|)^{1/2}$.AR reduces the Prandtl-Glauert equation of linearized aerodynamics to Laplace's equation for unsteady motion in the crossflow plane. Forces are the consequence of changing vortex system impulse, and the axial coordinate enters the formulation only as a parameter in boundary data. This theory applies equally well to subsonic or supersonic flows. In the supersonic regime, wing edges must be highly subsonic. When derived from the Prandtl-Glauert equation, slender body theory should be restricted to small angles, pointed configurations, and continuous body slopes, but some results may be extended to blunt planforms.[25] The same governing relations follow in incompressible and transonic flows with somewhat fewer restrictions. It is specifically for low speeds that the following theory is intended.

The governing equations to order ε^2 are

$$\partial^2\phi/\partial Y^2 + \partial^2\phi/\partial Z^2 = 0 \tag{1}$$

subject to uniform flow upward at velocity $U_\infty \sin\alpha$ far from the body and impermeability of the body surface. The coordinate system considered is given in Fig. 1.

Consider some station downstream of the apex of the wing. At this location vortices shed upstream are already present, and we investigate the flowfield into which an additional vortex is to be shed. The complex potential is

$$W = -iU_\infty \sin\alpha\left(\sigma - \frac{S^2}{4\sigma}\right) - \frac{i}{2\pi}\sum_{j=1}^{n}\Gamma_j \log\left[\frac{(\sigma-\sigma_j)(\sigma+S^2/4\sigma_j)}{(\sigma+\sigma_j)(\sigma-S^2/4\sigma_j)}\right] \tag{2}$$

where the physical plane ($\zeta = Y + iZ$) is related to the transformed variables by

$$\sigma = \tfrac{1}{2}[\zeta + (\zeta^2 - S^2)^{1/2}] \tag{3}$$

This transformation takes the wing cross section, a slit $-S \le \zeta \le S$, onto the circle $|\sigma| = S/2$. Vortices placed at image points insure satisfaction of boundary conditions, and the first terms in Eq. (2) are flow about a cylinder in the transform plane. Neither the locations nor strengths of the free vortices affect the "attached" flow. Similarly, attached flow contributions to forces will be independent of vortex strengths or locations to this order of approximation. This reflects the fact that incompressible flows are indeterminate by the total circulation, and that this circulation must be determined from subsidiary conditions based upon the existence of phenomena not inherent in the inviscid physical model.

It may be shown that velocities induced at any vortex location are finite everywhere except at the wing tips. Since viscosity will not permit large velocity gradients, we credit the creation of vorticity to the existence of viscosity and demand that a new vortex exists of sufficient strength to cause smooth outflow round the edge of the wing,

$$dW/d\sigma = 0 \quad \text{at} \quad \sigma = \pm S/2 \tag{4}$$

Hence

$$\Gamma_n \operatorname{Re}\left[\frac{\sigma_n}{\sigma_n^2 - S^2/4}\right] = \pi U_\infty \sin\alpha - \sum_{j=1}^{n-1}\Gamma_j \operatorname{Re}\left[\frac{\sigma_j}{\sigma_j^2 - S^2/4}\right] \tag{5}$$

An appropriate vortex strength may be found for any vortex location. That is, the Kutta condition is only one equation, and two more are required in order for both vortex strength and location to be determined.

In the method of Brown and Michael the two additional constraints are supplied by the requirement that the feeding sheet be of zero strength and that the sheet and concentrated vortex be force free in the mean. These assumptions are tantamount to specifying the rate at which vorticity is shed from the edge of the wing and the location of each vortex at the moment it is shed. Both of these may be determined experimentally and then employed in subsequent theories. This is often done, but Sacks et al.,[18] offer an interesting alternative.

Satisfaction of the Kutta condition eliminates velocities normal to the plane of the wing at the wing tip, thus each new vortex shed must initially move in that plane. This is true between chordwise control points; and, if these control points are close together, the vortices shed can move very little normal to the plane of the wing. If v_i is the velocity induced at the edge of the wing, all vortices will lie in a vortex sheet of width,

$$\delta = \int_x^{X+dX}\left(\frac{v_i}{U_\infty} - \frac{dS}{dX}\right)dX \tag{6}$$

The sheet width is determined by vortices previously shed since

$$v_i = -\frac{S}{\pi}\sum_{j=1}^{n}\Gamma_j \operatorname{Im}\left[\frac{\sigma_j^2}{(\sigma_j^2 - S^2/4)^2}\right] \tag{7}$$

contains no contribution from vortices in the plane of the wing.

The Kutta condition for previously shed vortices and a flat vortex sheet segment is

$$\int_{S/2}^{S/2+\delta_\sigma}\gamma(\sigma)\frac{d\sigma}{\sigma} = U_\infty \sin\alpha - \sum_{j-1}^{n-1}\Gamma_j \operatorname{Re}\left[\frac{\sigma_j}{(\sigma_j^2 - S^2/4)^2}\right] \tag{8}$$

where $S/2 + \delta_\sigma$ is the mapping of $S + \delta$ given by Eq. (6). The wing span will change little over the distance between successive chordwise control points, and each incremental vortex will be of nearly the same strength as all others shed in the differential axial distance of interest. If the vortex density is uniform, Eq. (8) provides the value of γ. Once this has been obtained, all vorticity in the sheet may be concentrated in a single vortex placed in the plane of the wing according to Eq. (5).

After a new vortex is shed, the entire vortex distribution must be allowed to move to the next chordwise station. All vortices are convected axially at velocity $U_\infty \cos\alpha$. Simultaneously they move in the crossflow plane under their own influence, that of the bound vortex system, and that due to the upward freestream. The crossflow velocity of the kth vortex is

$$\frac{d\bar{\zeta}_k}{dt} = \frac{i}{2\pi}\left(\frac{\sigma_k}{\zeta_k^2 - S^2}\right)\left[\sum_{j=1}^{n}\Gamma_j\left(\frac{1}{\sigma_k + \bar{\sigma}_j} - \frac{1}{\sigma_k - S^2/4\bar{\sigma}_j}\right) - \sum_{j\neq k}^{n}\Gamma_j\left(\frac{1}{\sigma_k - \sigma_j} + \frac{1}{\sigma_k + S^2/4\sigma_j}\right) - 2\pi U_\infty \sin\alpha - \frac{\Gamma_k}{\sigma_k + S^2/4\sigma_k}\right] + \frac{i\Gamma_k}{4\pi}\frac{S^2}{\sigma_k(\zeta_k^2 - S^2)} \tag{9}$$

The free vortex induced force borne by the chordwise wing segment of interest is the change in impulse of the vortex distribution in the axial distance involved,

$$\Delta N = 2\rho U_\infty \sum_{j=1}^{n}\Gamma_j \operatorname{Re}[(\zeta_j^2 - S^2)^{1/2}]\Big|_x^{x+\Delta X} \tag{10}$$

ΔN contains contributions due to the addition of new vortices as well as changes in impulse due to the motion of vortices already present. Since there are no vortices at the apex of a pointed planform, the quantity above evaluated at the trailing edge of a single surface would give the total separated force. Moments and stability derivatives may be calculated in the manner outlined by Sacks.[26]

As suggested by Adams and Sears,[24] at the trailing edge of the wing, vortices due to the attached flow are added to the

leading edge vortex system. Trailing edge vortices correspond to a spanwise loading which maintains the discontinuity in ϕ across the surface. The Kutta condition is not satisfied at the trailing edge, and consequences of the other trailing edge effects are ignored. Since the potentials of the leading edge vortices are discontinuous across the surface, the load is not elliptical,

$$\Delta\phi - \Delta\phi(0) = 2U_\infty \sin\alpha \cdot (S^2 - y^2)^{1/2} - \sum_{j=1}^{n} \mathrm{Re}\left\{\frac{i\Gamma_j}{2\pi} \log \times \left[\frac{i(S^2 - y^2)^{1/2} - (\zeta_j^2 - S^2)^{1/2}}{i(S^2 - y^2)^{1/2} + (\overline{\zeta_j}^2 - S^2)^{1/2}} \cdot \frac{i(S^2 - y^2)^{1/2} - (\overline{\zeta_j}^2 - S^2)^{1/2}}{i(S^2 - y^2)^{1/2} + (\zeta_j^2 - S^2)^{1/2}}\right]\right\} \tag{11}$$

Sack's method is attractive because it reveals the details of the flowfield. Since vortices follow streamlines, streamline patterns are available. Because the vorticity present is well distributed, spanwise loadings and downwash patterns are not unrealistically influenced by isolated strong vortices. Nowhere in the formulation need the origin of previously shed vortices be specified. Thus, one may trace vortices shed by a lifting surface as they pass over trailing portions of the vehicle of interest, and one may determine their influence upon subsequent vortex shedding. The Mangler-Smith method as modified by Levinsky and Wei[12] presents additional difficulties when surface interactions are considered. Sacks' method remains unchanged no matter what situation is of interest.

Implementation of the Method

The numerical method is not self-starting. The existence of vortices previously shed is necessary for its application. Several starting procedures were implemented. Sacks, et al.[18] assumed the initial vortex to be shed at half the freestream velocity component normal to the wing. In the present investigation it was alternatively assumed that the canard began as a conical flow while the wing was initiated according to Smith's extension of the Brown-Michael analysis into which the present author incorporated a pair of extraneous vortices of strengths equal to the total of all canard vortex pairs. As expected, if integration steps are sufficiently small, the starting process is rapidly forgotten. Small increments throughout the flowfield are expensive of computer time, thus extremely small integration steps are used only near the apex of each surface. The size of successive increments is increased parabolically—within the constraints of numerical stability—as integration proceeds.

Naturally, numerical inaccuracies must be present in any computational scheme. In spite of attempts to minimize the instabilities involved in vortex tracing as described earlier, difficulties were still encountered. These difficulties appeared mainly on the trailing surface at small separations, when downwash fields were comparable with the upward freestream. The first difficulty is a tendency for vortices to pierce the wing surface at high angles of attack when the vortex sheet is strong and its centroid is near the surface. The discrete nature of the model makes this inevitable, and a similar occurrence was noted by Hackett and Evans[5] in their study of wake behavior near a ground plane. The computational scheme monitors the progress of vortices as they approach the wing surface. When they are sufficiently close to the surface, velocities normal to the surface are suppressed, and the possibility of their passing through is eliminated. A second difficulty is that due to close approach of vortices to each other and possible piercing of the vortex sheet. The tendency of individual vortices to be "lost" from the sheet was discussed at great length by Rogers.[9] He blamed numerical inaccuracies for this occurrence, but the extensive numerical analysis performed in the course of this investigation confirms that this is not necessarily the case. This is the behavior physically to be expected of a number of discrete potential vortices, and it may be suppressed if viscous cores are incorporated in the vortices. Yager, et al.,[10] did this, but such cores have no theoretical justification since the resulting distributions of singularities do not satisfy Laplace's equation. Sheet crossing anomalies occur in vortices near the end of the vortex sheet. Since Smith[17] has observed that one convolution of the sheet in addition to a concentrated vortex constitutes an adequate description of the flowfield, when two vortices move within a small fraction of the local span of each other they are combined in a single vortex located at their centroid. This eventually leads to a vortex sheet description not unlike that of Mangler and Smith.[16] The motion of individual vortices along streamlines is equivalent to the discrete numerical vortex sheet model of those authors.

The width of the vortex sheet given in Eq. (6) will be positive only if shed vortices move outward more rapidly than the wing grows. Since there is no upstream influence, the vortex system at a given chordwise station cannot anticipate the rate of growth of the wing. If the wing should grow more rapidly than the vortex sheet segment, free vortices will move onto the wing. Since there can be no velocity components normal to the wing, such vortices will not be able to join the vortex sheet. Furthermore, vortices in the plane of the wing coincide with their images and cannot affect the remaining flowfield. When this occurs, there are many possible physical interpretations. One point of view is that shedding rate must be such that V_i/U_∞ is always at least equal to dS/dX if vortices are to be shed at all from the leading edge. If vortices do not move off of the wing edge, the Kutta condition requires that they be of zero strength. That is, the present configuration of existing vortices is fortuitously just sufficient to satisfy the Kutta condition. In some situations this is nearly true, and the addition of a vortex of zero strength is acceptable. Another possibility is that vortices are shed from elsewhere than the wing-tip or that secondary separation occurs. Since the method provides no logical choice for an alternative shedding location, this answer is difficult to implement. Still another interpretation is that rollup of even the small vortex sheet segment near the wing is important. If a vortex is even in infinitesimal distance from the edge of the wing, it will experience a velocity component normal to the plane of the wing. This motion of vortices has been ignored within the chordwise segment in which a given vortex is shed, but when V_i/U_∞ is close to dS/dX it is important and must be accounted for.

A final important consideration is the convergence of the method. One expects that the forces and flowfields predicted cease to change for all practical purposes as the number of vortices shed along the edge of lifting surface is increased. The results of Ref. 18 have been independently confirmed, and it has been found that for aspect ratios of less than unity approximately fifty vortex pairs are sufficient for the prediction of normal force. The vorticity shed at the trailing edge is adequately described by less than twenty vortex pairs, but when these seventy vortex pairs are added to the fifty or more required on the trailing surface, over one hundred simultaneous nonlinear ordinary differential equations must be solved. Although initial portions of the calculation proceed rapidly, computation time for successive increments increases manyfold. To expedite computation, canard leading edge vortices are combined in pairs as soon as the trailing edge of the canard is reached. This greatly reduces the computation necessary to determine the flowfield about the wing and has negligible influence on force and moment coefficients. It is felt that the present scheme is computationally efficient and that the most serious sources of error have been minimized. Each case considered would require approximately 5 minutes of CDC 6600 processor time.

Results and Discussion

The method previously described has been implemented on the USAF Academy Burroughs B5500 computer. Since this initial investigation is tutorial in nature, a wide range of conditions has been investigated with no great detail in any single situation. The problem has numerous parameters which preclude any major advantage in dimensional analysis. The parameters of interest are the aspect ratios (AR_c, AR_w), the ratio of characteristic dimensions of the surfaces (c_c/c_w), the horizontal and vertical spacing of the surfaces (s_h/c_c, s_v/c_c), and the angles of attack of canard and wing (α_c, α_w). Results to be presented employ aspect ratios of 0.5 for both surfaces and a wing whose area is four times that of the canard. Both surfaces have delta planforms. This configuration incorporates a realistic interaction within the constraints of slender body theory. The method is not limited to the planforms studied herein.

The influence of leading edge vortices upon normal force is shown in Fig. 2. The normal force coefficient is based upon the sum of canard and wing areas. Horizontal and vertical distances between canard and wing are both equal to one-fourth of the canard chord. Classical linear theory predicts that $C_N = (\pi/2)AR \sin\alpha$. When the surfaces are very far apart there will be little interaction between them, and C_N for the combination is the same as that for each surface. At $\alpha = 20°$ the presence of leading edge vortices leads to normal forces comparable with those of the attached flow. When the surfaces are allowed to interact in the manner noted, these forces are degraded by almost fifteen percent. The degradation of lift is enhanced as the surfaces approach each other.

In Fig. 3 the paths of vortex centroids are shown for an angle of attack of ten degrees. The canard leading edge vortex core describes a nearly straight path. Beyond the canard trailing edge the lateral centroid of the entire canard vortex system remains invariant until the wing is encountered. Even after the canard vortices pass the apex of the wing they are much stronger than wing vortices, and their motion is affected very little by the presence of the wing. Although the natural tendency is for canard vortex cores to move downward at a uniform rate relative to the upward component of the free-stream, flow up over the wing and around the wing leading edge vortices carries them very slightly upward. As wing span increases, the impulse of the nearly stationary canard vortices will decrease. Thus a degradation of lift on at least the forward portion of the wing must be expected even if the wing vortex system were unaffected by the canard. Since the canard vortex system forces vortices shed from the wing to be closer to the wing surface and farther outboard than would be the case without interaction, wing vortex system impulse would be reduced even if its total circulation were unaffected. As the canard vortices pass

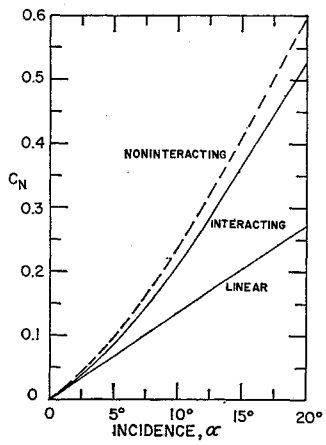

Fig. 2 Nonlinear normal force; $AR_C = AR_W = 0.5$, $S_V/C_C = S_H/C_C = 0.25$, $C_C/C_W = 0.5$, $\alpha_C = \alpha_W$.

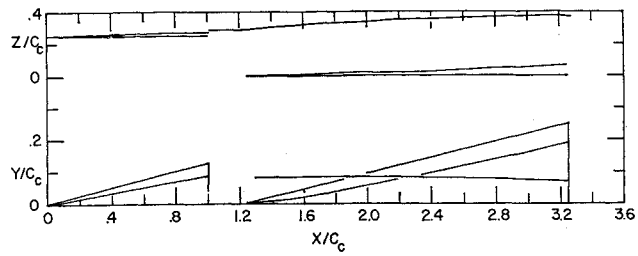

Fig. 3 Vortex centroid trajectories; $AR_C = AR_W = 0.5$, $S_V/C_C = S_H/C_C = 0.25$, $C_C/C_W = 0.5$, $\alpha_C = \alpha_W = 10°$.

over the wing vortex sheet, they are drawn inward and down toward the wing surface. This reduces lift both by decreasing canard vortex impulse and by forcing wing vortices outboard. There is a loss of lift to some extent over the entire wing. The loss of lift on forward portions of the wing moves the center of pressure toward the trailing edge. At the same time, wing lift is decreased relative to a wing unaffected by canard influences. The net result is a greater nose-up moment for the same normal force and thus a decrease in $|dC_m/dC_L|$ and in static longitudinal stability.

The detail which Sacks' method allows one to observe may be illustrated in nonconical flowfields. Several streamlines are shown in Fig. 4. Representative shapes of vortex sheets supported by the canard and wing are given in Figs. 5 and 6. Vortex sheet cross sections were obtained by connecting as many vortices as possible. In each figure over 90% of the vorticity present lies on the sheet as drawn. Nevertheless "old" vortices near the vortex centroid become quite confused and cannot logically be connected. Examination of Westwater's original figures reveals considerable

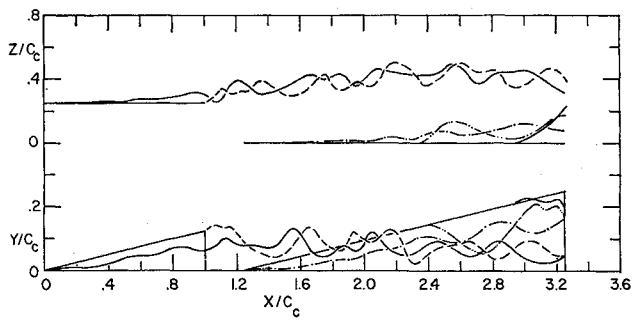

Fig. 4 Selected steamlines; $AR_C = AR_W = 0.5$, $S_V/C_C = S_H/C_C = 0.25$, $C_C = C_W = 0.5$, $\alpha_C = \alpha_W = 20°$.

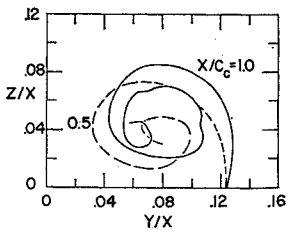

Fig. 5 Canard vortex sheet cross sections; $AR = 0.5$, $\alpha = 15°$.

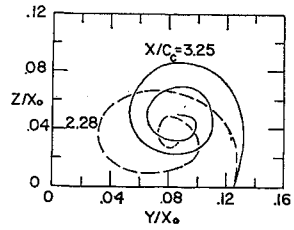

Fig. 6 Wing vortex sheet cross-section; $AR_C = AR_W = 0.5$, $S_V/C_C = S_H/C_C = 0.25$, $C_C/C_W = 0.5$, $\alpha_C = \alpha_W = 15°$.

imagination on the author's part when he connected the vortices. It is not important that one be able to perform this exercise as long as vortices are followed accurately. A distribution of discrete vortices need not remain coherent.

If one examines the canard vortex sheet cross sections shown, it is obvious that a conical flow has not been reproduced. If the flowfield were conical, each cross section would be similar to all others. Sacks et al.,[18] do not note such behavior in their original application of the method, but this phenomena must have appeared. Since vortex centroids describe nearly linear paths, and total circulation grows almost linearly, the intervals over which vortices are shed as well as the extent to which vortices are engulfed by a central core can greatly affect vortex sheet shapes. Furthermore, the vortex sheet near the trailing edge is composed of many more vortices than that near the apex and must exhibit greater detail. An analysis which assumes a conical flow must have equal numbers of vortices at each location. As Smith[21] has observed, there are really no subsonic conical flows. Although experiments suggest that circulation is nearly linear with axial distance, this cannot strictly be true. The present analysis does not assume that the flow be conical, and results indicate that it is nearly, but not exactly, so. Particularly near the apex, vorticity is shed at somewhat less than the rate predicted by conical analyses. This is consistent with what occurs physically, since conical flow analyses almost universally overpredict separation induced normal forces. It has been confirmed that this phenomenon is not numerical since decreasing step size has little effect. The method may, however, be inherently at fault. Integrated properties indicate a nearly conical flow with center of pressure between 68 and 69% of the chord from the apex (depending upon angle of attack).

The effect of wing-canard misalignment is indicated in Fig. 7. There it is shown that when the canard is at a greater angle of attack than the wing, the total normal force on the configuration may be less than when the canard is at a smaller angle of attack than the wing. The reason for this is the inhibition of wing vortex shedding when canard vortices are nearby. When canard vortices are near the wing, the Kutta condition does not require as strong a vortex as when canard vortices are farther away. The wing sees a locally reduced angle of attack because of canard downwash. If canard vortices are weakened, then wing vortices must be stronger, and this is illustrated in the figure. Thus, the wing may gain more lift than the canard loses when canard incidence is decreased. Since most of this gain is on rearmost portions of the wing, the center of pressure moves farther rearward than would be anticipated on the basis of a noninteracting analysis. Deflection of the canard directly affects the wing loading. This effect is adverse for maneuverability since canard deflection results in neither forces nor moments of the magnitude predicted by a noninteracting analysis. Nevertheless, direct control of wing loading is exactly what is required of control configured aircraft. In fact, the figure demonstrates that in this case there is a range of canard misalignment wherein canard gains and wing losses are

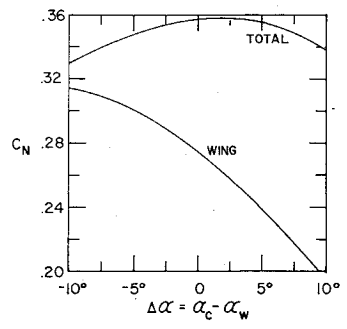

Fig. 7 Effect of canard misalignment; $AR_C = AR_W = 0.5$, $S_V/C_C = S_H/C_C = 0.25$, $C_C/C_W = 0.5$, $\alpha_W = 15°$.

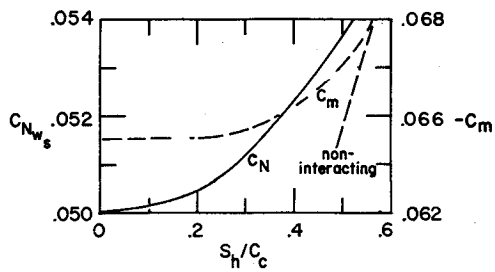

Fig. 8 Effect of horizontal separation; $AR_C = AR_W = 0.5$, $S_V/C_C = 0.25$, $C_C/C_W = 0.5$, $\alpha_C = \alpha_W = 10°$.

nearly balanced and the main effect is center of pressure motion.

In order to assess the utility of the present method in design studies, a systematic investigation of the effect of canard-wing separation was undertaken. The effect of changing horizontal separation upon separation induced normal force is shown in Fig. 8. The vertical separation is maintained at 25% of the canard chord. Degradation of wing lift is less the greater the extent of rollup of the canard vortex sheet. When distributed canard vorticity interacts directly with the wing without any rollup, wing lift is degraded most. Therefore, flat wake analyses lead to conservative values of total lift while fully-rolled up analyses will underpredict the effects of interaction. When there is no interaction, C_m will increase in proportion to the increase in canard-wing horizontal separation. When the interaction is included, forward motion of the canard is accompanied by increased lift on the wing, and pitching moment will not decrease as much as a noninteracting analysis would predict. Eventually, dC_m/dS_h approaches its noninteracting value.

The effect of vertical separation is shown in Fig. 9. Horizontal separation is maintained at 25% of the canard chord. The separation induced normal force has a broad minimum which begins at nearly that separation for which canard vortices first intersect the plane of the wing. More than two-thirds of the noninteracting normal force due to wing leading edge vortices may be lost. For the horizontal separation chosen, wing lift is almost invariant over a fairly wide range of vertical separations.

The origin of the large decreases in normal force on the wing is depicted in Fig. 10. Horizontal separation of the surfaces is 0.25 C_c as before, and the variation of wing circulation with vertical separation is shown. As the canard approaches the plane of the wing, the vortex shedding rate $(d\Gamma/dX)$ decreases. At extremely small separations, the downwash field of the canard is so strong that the forward portion of the wing sees a flow which is actually opposite to the upward stream, and shedding of vortices of negative sense is necessary. As wing span grows, the effect of downwash of the canard vortices upon the wing is reduced, and eventually vortices of positive sense are shed. The vortex sheet will tear when the sense of shed vortices changes. The actual lift producing

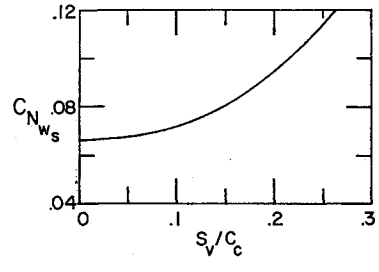

Fig. 9 Effect of vertical separation; $AR_C = AR_W = 0.5$, $S_H/C_C = 0.25$, $C_C/C_W = 0.5$, $\alpha_C = \alpha_W = 15°$.

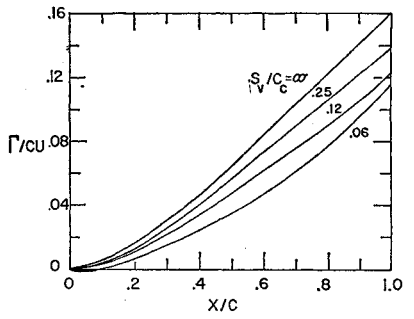

Fig. 10 Effect of vertical spacing on circulation; $AR_C = AR_W = 0.5$, $S_H/C_C = 0.25$, $C_C/C_W = 0.5$, $\alpha_C = \alpha_W = 15°$.

vortex sheet emanates from someplace downstream of the wing apex. The effect of small vertical separations is further illustrated in Fig. 11 wherein the normal force coefficients due to leading edge vortices on canard and wing are given. The departure from conical flow on the canard is extremely small, and the normal force varies nearly parabolically. The separation induced normal force is distinctly different and is negative over a rather large portion of the wing. Indeed on the most forward portions of the wing, the loading due to vortices of negative sense and reduced canard vortex impulse can be comparable with the attached flow loading. When vertical spacing is very small relative to the chord of the canard, the forward portion of the wing will be detrimental to overall lift. If this portion of the wing were eliminated, canard vortices would move farther before encountering the wing and their effect would be less detrimental. At any rate, a nonlifting wing segment is of no use. It is conjectured that this is perhaps one reason for the planform chosen for the SAAB Viggen. These phenomena are confirmed in Ref. 27.

The appearance of vortices of negative sense is not without precedent. Smith[14] has observed decreasing shedding rates upon a class of nonconical planforms and has justified their existence theoretically although he doubts their existence on planforms of nonzero thickness. Thwaites[28] notes that on some slender wings, vorticity shed from part of the trailing edge may be of opposite sense and cites observations which prove the existence of this phenomenon. It is entirely possible that the phenomenon reported above does exist in the real flowfield which has been modeled. The theory of Brown and Michael has been formulated by the present author in the presence of free vortices, and it has been confirmed that it too will predict vortices of negative sense in a strong downwash field. Kuhn, et. al.,[15] report decreasing shedding rates upon cones in lunar motion but dismiss their observations as being physically unrealistic. Since phenomena observed in the design of the SAAB Viggen have been reproduced at least qualitatively, the model employed describes the physical aspects of the flowfields of interest adequately.

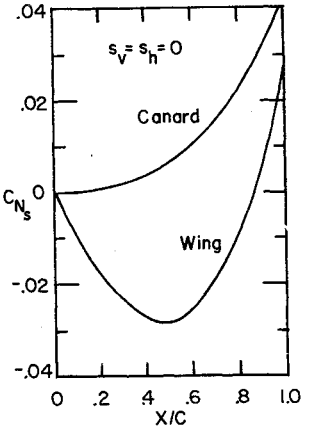

Fig. 11 Separation induced normal force; $AR_C = AR_W = 0.5$, $S_V/C_C = S_H/C_C = 0.0$, $C_C/C_W = 0.5$, $\alpha_C = \alpha_W = 15°$.

Conclusions

Sacks' description of vortex shedding at the edges of slender wings has been applied to the study of the interaction of close-coupled delta wing-canard configurations. The approach permits distortion of the canard wake as it interacts with the wing. The canard affects wing lift adversely. The greater the extent to which canard vortex sheets are rolled up, the less is the adverse effect. Lift curve slope is reduced relative to that of noninteracting surfaces, and static longitudinal stability is decreased. Vortices of negative sense may be shed when a canard is very close to the wing, and the forward portion of a slender wing in close proximity to a canard surface is ineffective in producing lift.

The method is shortly to be applied to the study of the importance of vortex shedding in the operation of low-aspect ratio, ram-wing ground effect vehicles. An optimization of spacings and planforms for wing-canard configurations is also to be attempted. The ease of application of Sacks' approach to arbitrary configurations is quite attractive.

References

[1] Jenkins, J. E., Eckholdt, D. C., and Kujawski, B. T., "An Assessment of the Interfacing Problems Associated with CCV Design Concepts," AIAA Paper 70-926, Los Angeles, Calif., 1970.

[2] Landahl, M. T. and Stark, V. J. E., "Numerical Lifting-Surface Theory—Problems and Progress," *AIAA Journal*, Vol. 6, No. 11, Nov. 1968, pp. 2049–2060.

[3] Carlson, H. W. and Harris, R. V. Jr., "A Unified System of Supersonic Aerodynamic Analysis," *Analytic Methods in Aircraft Aerodynamics*, NASA SP-228, 1969, pp. 639–658.

[4] Spreiter, J. R. and Sacks, A. H., "The Rolling-Up of the Trailing Vortex Sheet and Its Effect on the Downwash Behind Wings," *Journal of the Aeronautical Sciences*, Vol. 18, No. 1, Jan. 1951, pp. 21–32.

[5] Hackett, J. E. and Evans, M. R., "Vortex Wakes Behind High-Lift Wings," *Journal of Aircraft*, Vol. 8, No. 5, May 1971, pp. 334–340.

[6] Westwater, F. L., "Rolling-Up of the Surface of Discontinuity Behind an Aerofoil of Finite Span," R & M 1962, 1935, British ARC.

[7] Batchelor, G. K., *An Introduction to Fluid Dynamics*, Cambridge University Press, Oxford, 1967, pp. 580–593.

[8] Sacks, A. H., "Vortex Interference of Slender Airplanes," TN-3525, 1955, NACA.

[9] Rogers, A. W., "Application of Two-Dimensional Vortex Theory to the Prediction of Flow Fields Behind Wings of Wing-Body Combinations at Subsonic and Supersonic Speeds," TN-3227, 1959, NACA.

[10] Yager, P. M., Holland, C. H., and Strand, T., "Modified Weissinger Lifting Surface Method for Calculating Aerodynamic Parameters of Arbitrary Wing-Canard Configurations," Rept. 354, Aug. 1967, Air Vehicle Corporation, La Jolla, Calif.

[11] Polhamus, E. C., "A Concept of the Vortex Lift of Sharp-Edge Delta Wings Based on a Leading Edge Suction Analogy," TN-D-3767, 1969, NASA.

[12] Levinsky, E. S., Wei, M. H. Y., and Maki, R. L., "Theoretical Studies of Vortex Flow on Slender Wing-Body Combinations," *Analytic Methods in Aircraft Aerodynamics*, NASA SP-228, 1969, pp. 638–702.

[13] Brown, C. E. and Michael, W. H. Jr., "Effects of Leading-Edge Separation on the Lift of a Delta Wing," *Journal of the Aeronautical Sciences*, Vol. 21, No. 10, Oct. 1954, pp. 690–694; also TN 3430, NACA.

[14] Smith, J. H. B., "A Theory of the Separated Flow from the Curved Leading Edge of a Slender Wing," R & M 3116, 1957, British ARC.

[15] Kuhn, G. D., Spangler, S. B., and Nielson, J. N., "Theoretical Analysis of Vortex Shedding from Bodies of Revolution in Coning Motion," *AIAA Journal*, Vol. 9, No. 5, May 1971, pp. 784–790; also, CR-1448, NASA.

[16] Mangler, K. W. and Smith, J. H. B., "A Theory of the Flow Past a Slender Delta Wing with Leading Edge Separation," *Proceedings of the Royal Society*, Ser. A, Vol. 251, 1959, pp. 200–217.

[17] Smith, J. H. B., "Improved Calculations of Leading-Edge Separation from Slender, Thin, Delta Wings," *Proceedings of the Royal Society*, Ser. A, Vol. 306, 1968, pp. 67–90.

[18] Sacks, A. H., Lundberg, R. E., and Hanson, C. W., "A Theoretical Investigation of the Aerodynamics of Slender Wing-Body Combinations Exhibiting Leading-Edge Separation," CR-719, 1967, NASA.
[19] Murty, G. S. and Sankara-Rao, K., "Numerical Study of a System of Parallel Line Vortices," *Journal of Fluid Mechanics*, Vol. 40, Pt. 3, Feb. 1970, pp. 595–602.
[20] Margason, R. J., "Analysis of the Flow Field of a Jet in a Subsonic Crosswind," *Analytic Methods in Aircraft Aerodynamics*, NASA, SP 228, 1969.
[21] Beavers, G. S. and Wilson, T. A., "Vortex Growth in Jets," *Journal of Fluid Mechanics*, Vol. 44, Pt. 1, Oct. 1970, pp. 97–112.
[22] Smith, J. H. B., "Theoretical Work in the Formation of Vortex Sheets," *Progress in the Aeronautical Sciences*, Vol. 7, edited by D. Kuchemann, Pergamon, 1966, pp. 35–51.
[23] Ashley, H. and Landahl, M., *Aerodynamics of Wings and Bodies*, Addison-Wesley, Reading, Mass., 1965, pp. 99–119.
[24] Adams, M. C. and Sears, W. R., "Slender Body Theory—Review and Extension," *Journal of the Aeronautical Sciences*, Vol. 20, No. 2, Feb. 1953, pp. 85–98.
[25] Lagerstrom, P. A. and Graham, M. E., "Remarks on Low Aspect Ratio Configurations in Supersonic Flow," *Journal of the Aeronautical Sciences*, Vol. 18, No. 2, Feb. 1958, pp. 91–96.
[26] Sacks, A. H., "Aerodynamic Forces, Moments, and Stability Derivatives for Slender Bodies of General Cross-Section," TN 3283, 1954, NACA.
[27] Behrbobm, H., "Basic Low Speed Aerodynamics of the Short-Coupled Canard Configuration of Small Aspect Ratio," TN 600, 1965, SAAB, Linkoping, Sweden.
[28] Thwaites, B., *Incompressible Aerodynamics*, Clarendon Press, Oxford, 1960, pp. 508–516.

JUNE 1972 J. AIRCRAFT VOL. 9, NO. 6

Drift of Buoyant Wing-Tip Vortices

ROBERT C. COSTEN*
NASA Langley Research Center, Hampton, Va.

An exact solution is derived for the trochoidal motion of a single horizontal buoyant vortex drifting under gravity, and a criterion is given for such vortices to persist. Approximate solutions are obtained for the two-dimensional drift of buoyant wing-tip vortices descending in a neutrally stable atmosphere where the buoyancy is achieved by injecting hot gas from the engine exhaust or auxiliary burners into the vortex cores. The vortices are found to approach each other as they descend. This effect may accelerate their breakup and thus reduce the period of time when the wake from a large aircraft is dangerous to other aircraft. At low altitudes the ground effect may dominate and cause buoyant wing-tip vortices to separate instead of approach each other. Formulas and graphs are presented for calculating these effects, and sample calculations are applied to the Boeing 747 aircraft. A weakly stable atmosphere should increase the buoyancy and the convergence rate of descending wing-tip vortices, and a method is presented for calculating the combined effect of core heating and atmospheric stability.

Nomenclature

A = cross-sectional area of a buoyant vortex core which contains the vorticity and buoyant fluid, m^2
a = nominal radius of oval core of a buoyant vortex, such that $A = \pi a^2$, m
b = initial separation of trailing vortices upon roll-up several wing-spans downstream of aircraft, m
g = gravitational acceleration, m/sec^2
P = downward momentum (or impulse) per unit length of a trailing vortex pair, kg-m/sec
p = pressure, N/m^2
$\mathbf{R}$ = (X, Y) position vector in two dimensions of the center of mass of a buoyant vortex core, m
$\mathbf{R}_\omega$ = center of circulation of a vortex, m
$\mathbf{r}$ = (x,y) position vector in two dimensions, m
S = area of integration, m^2
T_F = stagnation temperature of the fan exhaust from a fanjet engine, °K
T_o = temperature of the standard atmosphere, °K
T_P = stagnation temperature of the primary engine exhaust from a fanjet engine, °K
t = time, sec
$\mathbf{U}$ = velocity of displacement of vorticity such that the circulation on any circuit which moves with velocity $\mathbf{U}$ remains constant, m/sec
$\mathbf{v}$ = fluid velocity, m/sec
$\mathbf{v}_\infty$ = uniform flow velocity, m/sec
W_P = mass flux through the primary engine of a fanjet, kg/sec
W_F = mass flux through the fan of a fanjet engine, kg/sec
w = relative forward airspeed, m/sec
X, Y = Cartesian coordinates for the center of mass of a buoyant vortex in two dimensions, m
Y_m = minimum altitude of an aircraft below which the ground effect dominates and buoyancy will not bring its trailing vortices closer together, m
x,y = Cartesian coordinates in two dimensions, m
$\hat{z}$ = unit vector perpendicular to the x-y plane and parallel to the vorticity vector in two dimensions
Γ = circulation of a vortex, m^2/sec
κ = $\Gamma^2/2\pi^2a^2bg$ dimensionless parameter
λ = buoyancy index defined by equation (4)
ρ = fluid density, kg/m^3
ρ' = a constant, or a single-valued function of the pressure, kg/m^3
ρ_o = density of the standard atmosphere, kg/m^3
τ = contact time for wing-tip vortices made buoyant by initial core heating in a neutrally stable atmosphere, defined as the time after generation for the vortex cores to drift into uniform tangential contact, sec

Presented as Paper 71-604 at the AIAA 4th Fluid and Plasma Dynamics Conference, Palo Alto, Calif., June 21–23, 1971; submitted July 9, 1971; revision received February 7, 1972.
Index categories: Airplane and Component Aerodynamics; Jets, Wakes, and Viscid-Inviscid Flow Interactions; Hydrodynamics.
* Aero-Space Technologist, Space Physics Branch, Environmental and Space Sciences Division.